



Supercritical CO₂ applications in microfluidic systems

Aslihan Kazan¹

Received: 17 June 2022 / Accepted: 8 August 2022 / Published online: 16 August 2022
© The Author(s), under exclusive licence to Springer-Verlag GmbH Germany, part of Springer Nature 2022

Abstract

Supercritical fluid technology has been used for a variety of applications for decades and received special attention in the fields of analytics, extraction and purification of valuable compounds and preparation of drug carriers. Among supercritical fluids, supercritical CO₂ is the most attractive one as being nontoxic, nonflammable and chemically inert. In addition, the critical temperature and pressure of CO₂ is quite moderate which makes supercritical CO₂ a popular solvent for a wide range of applications from laboratory to industrial scale. In recent years, a promising research field called as supercritical microfluidics was developed to merge the advantages of supercritical fluids and microfluidics, the science and technology of manipulating liquids in extremely small volume. This review discusses the recent progress in supercritical microfluidics with a focus on supercritical CO₂, the most commonly used solvent in supercritical fluid processes, and some applications of supercritical CO₂ in microscale such as extraction of valuable compounds, determination of dissolution characteristic in various solvents, performing chemical reactions and particle synthesis are presented.

Keywords Microfluidics · Supercritical fluids · Carbon dioxide · Microreactor · Fabrication

1 Introduction

Microfluidic systems are three dimensional structures consisting of micron-size (10–1000 μm) channel networks at different geometries and enable to handle liquids in extremely small volumes (Coyle and Oelgemöller 2008; Theberge et al. 2010). High surface area to volume ratio and short diffusion distances in microfluidic systems allow to reach enhanced mass and heat transfer and faster reaction rates which are not approachable in traditional batch systems (Teh et al. 2008). As a result of laminar flow in microchannels, microfluidic systems are operated with different flow scenarios like parallel, plug flow or slug flow and reaction conditions are highly controlled (Krühne et al. 2014; Qian et al. 2019). By taking these advantages, several potential applications of microfluidic systems such as conducting reactions with explosive and hazardous reagents and products (Janicke et al. 2000; Palde and Jamison 2011), reducing the consumption of expensive reagents (Liu et al. 2003) and

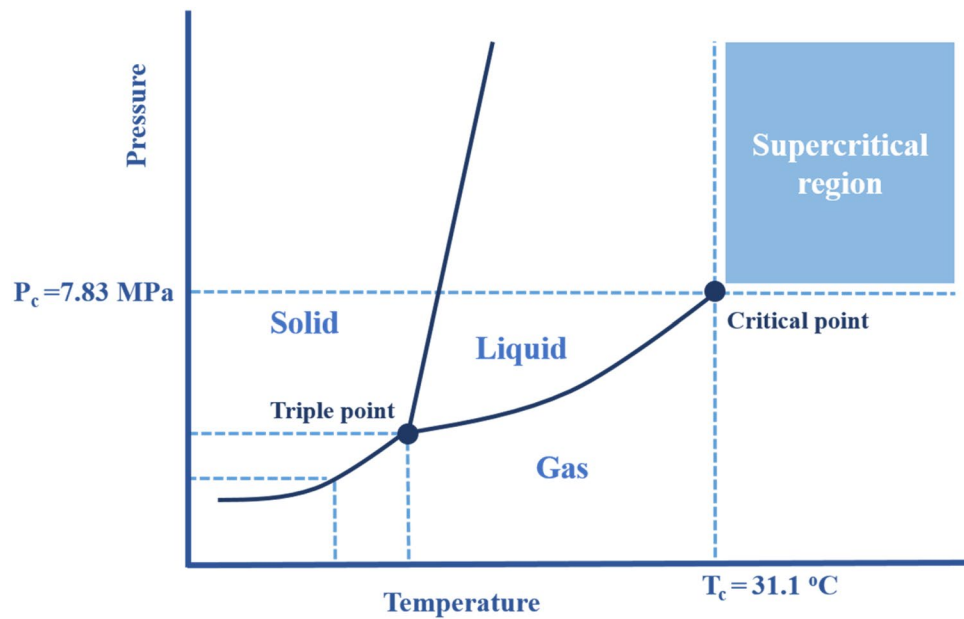
performing exothermic reactions with fast energy transfer demand (Antes et al. 2003; Wang et al. 2011) are reported.

A supercritical fluid is defined as a substance with pressure and temperature above the critical values and has both liquid and gas-like properties (Blanchard and Brennecke 2001). Supercritical fluids have liquid-like density, gas-like viscosity and diffusivity and their density can be easily tuned by small pressure changes in the critical region (Nalawade et al. 2006).

CO₂ is the most commonly used solvent in supercritical fluid applications as it is cheap, nontoxic, nonflammable, chemically inert, classified as generally recognized as safe and has convenient critical values such as critical pressure of 7.383 MPa and critical temperature of 31 °C (Fig. 1) (Williams et al. 2002; Tyśkiewicz et al. 2018; Yahya et al. 2018; Zhu et al. 2018). Having a critical temperature quite lower than most commonly used solvents such as ethanol ($T_c = 240.9$ °C), methanol ($T_c = 239.6$ °C), acetone ($T_c = 235.1$ °C) and water ($T_c = 374.1$ °C) makes CO₂ more advantageous particularly in terms of energy requirement of the process and thermal destruction of valuable compounds (Sahena et al. 2009). Besides these properties, easier downstream processing like removing from the system by simple depressurization, higher stability and more environment friendly nature makes supercritical CO₂ more advantageous

✉ Aslihan Kazan
kazanaslihan@gmail.com

¹ Department of Bioengineering, Faculty of Engineering and Natural Sciences, Bursa Technical University, Bursa, Turkey

Fig. 1 Phase diagram of CO₂

than organic solvents (Leitner 2002). Supercritical CO₂ has been widely used in various applications such as extraction of bioactive compounds from various natural sources (Mendes et al. 2003; Uwineza and Wańkiewicz 2020), supercritical fluid chromatography as an analytic tool (Taylor 2009), an environmentally benign reaction medium for catalysis (Leitner 2002), production of biofuels (Boock et al. 2019), polymer synthesis and modification (Nalawade et al. 2006), production of nanomaterials like nanoparticles and nanocellular foams for pharmaceutical and medical purposes (Reverchon and Adami 2006), using as a medium for dyeing of textiles without the need of drying (Knittel et al. 1993), degreasing, fiber separating and tanning in leather processing with reduced ecological burden (Hu and Deng 2016), gelation of biopolymers (Gurikov et al. 2015), drying of hydrogels to obtain aerogels (Tang and Wang 2005; Brown et al. 2010), preparation of scaffolds for tissue engineering applications (Kumari and Dutta 2010; Pisanti et al. 2012).

Supercritical microfluidics is a recently developed field combining the advantages of supercritical fluids and microfluidics (Ciceri et al. 2014). One of the advantages of microfluidic systems is the efficient mixing characteristic. Ionic liquid and CO₂ mixture is a new green solvent system for the separation and purification of chemicals and natural products. Since the density difference between the ionic liquids and CO₂ and also the higher viscosity of ionic liquids, it is difficult to mix two phases using traditional equipments. Qin et al. (2018a, b) developed a micromixer based on passive mixing technology to mix supercritical CO₂ and a representative ionic liquid, 1-ethyl-3-methylimidazolium tetrafluoroborate ([Emim][BF₄]). The system consisted of a T-junction and a tube both made by stainless steel and

the inner diameters were 0.75 mm. The system was operated under different temperature (308–343 K) and pressure values (0.1–15 MPa) and the effects of CO₂ and ionic liquid flow rates and flow rate ratio on the bubble formation were examined. It was shown that bigger bubbles were obtained at higher CO₂/ionic liquid flow rate ratio and supercritical CO₂ bubbles with average diameter between 0.3–1.2 mm with lower polydispersity indexes than 35% were prepared successfully.

2 Characteristics of supercritical fluids in microscale

Supercritical microfluidics combines the advantages of supercritical fluids and liquid microfluids (Fig. 2). In microchannels, fluid flow is characterized as laminar flow with low Reynolds number. The Reynolds number, the ratio of inertial forces to viscous forces, gives an information on the characteristics of fluid (density and viscosity) and the environment (fluid velocity and characteristic dimension) where the fluid flows (Elvira et al. 2013). As the physicochemical properties of supercritical fluids such as density and viscosity can be easily manipulated by the variation of temperature and pressure, the flow regime of a supercritical fluid in a microchannel can be tuned from laminar to turbulent. The friction factor and heat transfer coefficient values significantly differ in two flow regimes and directly affect the performance of the system. Not only the Reynolds number but also the angle between the channels in merging points, the roughness and geometry of channels affect the transition from laminar to turbulent

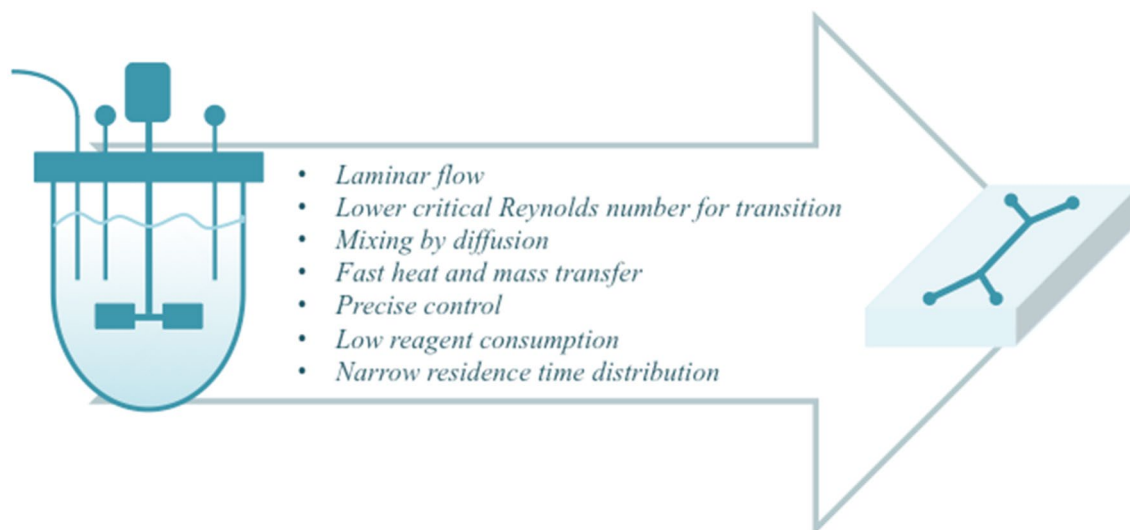


Fig. 2 Main advantages of microfluidic systems over conventional reactors

flow in microscale (Morini et al. 2009). Although the transition from laminar to turbulent flow occurs for the Reynolds number around 2000 in conventional systems, the critical Reynolds number is lower in microfluidic systems. Different critical values for laminar to turbulent transition between 200–900 were reported and it was showed that the hydraulic diameter of a microchannel significantly affects the critical Reynolds number differently from conventional systems (Peng and Peterson 1996; Pohar and Plazl 2008).

Mixing in microchannels is dependent on the diffusion between the fluids since the fluid flow is generally in laminar regime. To enhance the mixing of fluids, various passive or active micromixers were developed (Karimi et al. 2021). However, systems become more complex by the addition of these mixers and their characterization is also challenging. Segmented liquid–liquid or gas–liquid flows also provide enhanced mixing and the main advantage is that the mixing can be achieved in non-pattern, regular microchannels and an additional fabrication step for the micromixers is not required (Günther and Jensen 2006). The mixing time in a microchannel is a function of flow width and diffusion coefficient. In general, the diffusion coefficients of molecules in supercritical fluids are higher than in liquids (at least two orders of magnitude) which results in better mixing and lower mixing time for supercritical microfluidics compared to liquid microfluidics (Marre and Jensen 2010). In addition, the low viscosities of supercritical fluids also reduce the mixing time and enable the narrower residence time distribution which increases the yield of chemical reactions or enhances the product quality of particle synthesis conducted in microchannels (Song et al. 2006; Marre et al. 2008; Mou et al. 2022).

3 Physical dissolution of CO₂ in different solvents in microscale

The knowledge of dissolution behavior of CO₂ in different solvents, the equilibrium between two phases and mass transfer in multi-phase systems are important to design a high-pressure system and to understand and optimize the CO₂ reactions. In conventional systems, samples are physically taken from the system for the analysis which disturbs the phase equilibrium. The requirement for the depressurization, cleaning, refilling and pressurization after each sampling makes the system material and time consuming. Combining microfluidic systems with optical measurement methods such as ultraviolet (UV), near-infrared, fluorescence or Raman spectroscopy enables the continuous monitoring and data acquisition (Table 1) (Stratmann and Schweiger 2002; Adami et al. 2013).

A method was developed for the economic and fast determination of binary and ternary vapor–liquid equilibrium in a microcapillary using a Raman spectroscopy (Fig. 3a). The system was operated under high pressure ranging from 6 to 10 MPa for one binary and two ternary systems consisted of acetone–CO₂, acetone–CO₂–water and acetone–CO₂–N₂, respectively. It was shown that the obtained results for binary and ternary mixtures were in agreement with literature data and the combination of microfluidic technology and Raman spectroscopy can provide reliable data without taking samples and also reduce the equipment and chemical costs (Luther et al. 2015). Blanch-Ojea et al. (2012) used a non-adiabatic microfluidic T-junction with a semicircular cross section to investigate the effect of temperature and pressure on the behavior of CO₂–ethanol and CO₂–methanol systems and an inverted microscope with a CCD-high speed camera

Table 1 CO₂ dissolution in different solvents in microscale

Microreactor	Mixtures	Conditions	Measurement method	Reference
Borofloat glass microfluidic chip	CO ₂ –Ethanol CO ₂ –Methanol	7–18 MPa 294–474 K	Inverted microscope with CCD high-speed camera	Blanch-Ojea et al. (2012)
Silica capillaries	CO ₂ –Water	8–16.5 MPa 20–50 °C	Binocular microscope with high-speed camera	Guillaument et al. (2013)
Y-channel glass microfluidic system	CO ₂ –Water	10 MPa 50 °C	High-speed camera	Ogden et al. (2014)
Polyimide coated glass capillaries and stainless steel T-crossing	Acetone–CO ₂ Acetone–CO ₂ –Water Acetone–CO ₂ –Nitrogen	6–10 MPa 303–333 K	Phase selective Raman spectroscopy	Luther et al. (2015)
Double Y-channel glass microchip	CO ₂ –Water	11.4 MPa 40 °C	High-speed camera	Knaust et al. (2016)
Borosilicate glass microfluidic chip	CO ₂ –Brine	7.45 MPa 35 °C	Digital camera	Zheng et al. (2017)
Combination of OSTEMER and glass	CO ₂ –Ethanol	4.5–9 MPa 40 °C	High-speed camera	Martin et al. (2018)
Glass microfluidic chip	CO ₂ , Nitrogen or Water in decane	10 MPa 50 °C	Fluorescence microscope with digital camera	Nguyen et al. (2018)
T-junction silicon-glass microchip	CO ₂ –Water	8.5–9.5 MPa 35 °C	Inverted microscope with high-speed camera	Ho et al. (2021a)
PDMS channel in a metal platform	CO ₂ –Water	6.5 MPa 23.5 °C	Inverted microscope with high-speed camera	Ho et al. (2021b)
Silica capillaries embedded in epoxy	CO ₂ –Water	10 MPa 303 K	High-speed camera	Deleau et al. (2022)

was used for the image recording. Based on the applied temperature and pressure, CO₂ was in liquid, gas or supercritical state and vapor–liquid equilibrium with separated phases or a single phase was obtained. For vapor–liquid equilibrium Taylor, annular and wavy flow regimes were observed and temperature was shown to be more determinant than pressure on the system. In another study, a numerical approach was developed for the modeling of CO₂ and water flow in a microchannel under high pressure conditions. The surface wettability was changed from hydrophilic to hydrophobic by the variation of contact angle and a continuous water phase with CO₂ droplets was obtained for hydrophilic state while water droplets were observed in a continuous CO₂ flow for hydrophobic surface that indicated the strong effect of contact angle on the final hydrodynamic structures shape (Guillaument et al. 2013). The influence of surface modifications on microflows of supercritical CO₂ and water was investigated by Knaust et al. (2016). A double Y-channel glass microchip was used as uncoated or coated (with hydrocarbon or fluorocarbon) forms with different wettings. The results showed that an increased control can be achieved for either segmentation or parallel flow with surface modifications. The effect of flow rate and relative flow rate on the flow regime of supercritical CO₂–liquid water system was evaluated in a borosilicate glass microfluidic system with a Y-channel. The segmented flow was observed even at high flow rates as a result of low viscosity of supercritical

CO₂ and at the bifurcating exit of the microfluidic system, the splitting of supercritical CO₂ droplets was shown to be affected by wetting characteristics, total flow rate and droplet length while water plugs showed no such dependence (Fig. 3b, c) (Ogden et al. 2014). Martin et al. (2018) studied the hydrodynamics of CO₂–ethanol flow in a microchannel under high pressure conditions and investigated the effect of pressure and CO₂–ethanol composition on the developed flow regime. The results showed that different flow regimes namely two-phase Taylor flow, dissolving Taylor flow, single-phase jetting-dissolving flow and single-phase supercritical jetting-flow depending on the pressure and mixture composition. The Taylor bubble size was also affected by pressure and mixture composition as a result of changes the density and CO₂ mass flow rate, respectively. The bubble size increased with increasing CO₂ velocity at ambient conditions but decreased in the channel before reaching the equilibrium as CO₂ dissolves in ethanol. Most common flow patterns in microchannels were illustrated in Fig. 3d–g.

The knowledge of the CO₂ dissolution in different solvents is also applicable for the studies on deep geological formations since the ocean and sedimentary rocks are the main CO₂ reservoirs. The field studies of CO₂ dissolution and solubility are expensive and time consuming. However, it is possible to mimic the different environmental conditions using microfluidic systems (Abolhasani et al. 2014). Qin et al. (2018a, b) used a micro T-junction to investigate the

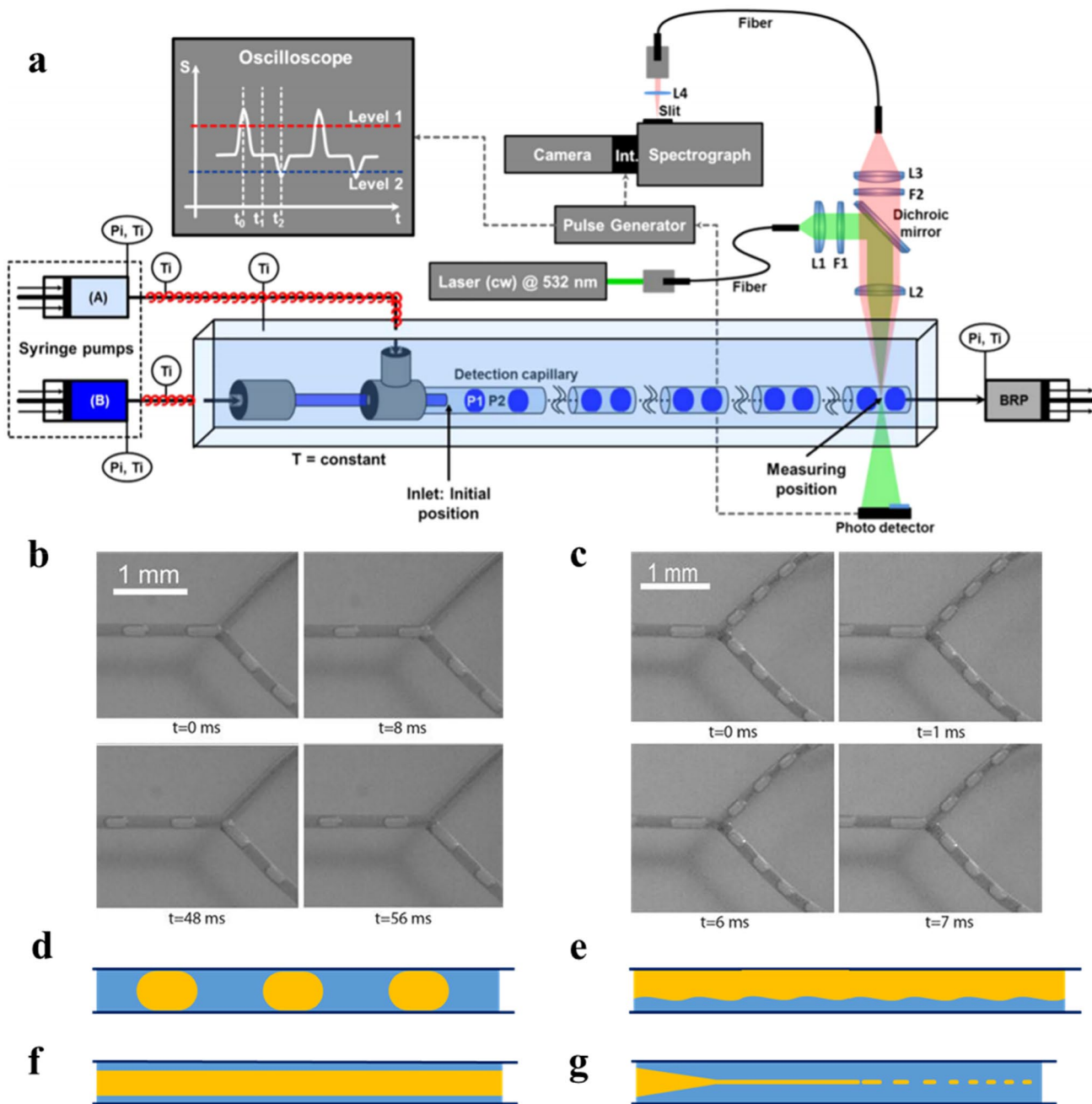


Fig. 3 a Scheme of a micro capillary combined with Raman spectroscopy to determine vapor–liquid equilibrium, reproduced with permission (Luther et al. 2015) from ACS. Splitting behaviour at bifurcating

exit of a microsystem for **b** 20 $\mu\text{L}/\text{min}$ and **c** 160 $\mu\text{L}/\text{min}$, reproduced with permission (Ogden et al. 2014) from Springer. Common flow patterns in microchannels: **d** Taylor, **e** wavy, **f** annular, **g** jetting-flow

shrinkage behavior of flowing supercritical CO_2 microdroplets in a water-carrier flow inside a straight microchannel for the applications on deep underground or oceanic CO_2 storage. Nguyen et al. (2018) investigated the effectiveness of nitrogen and supercritical CO_2 in the huff-and-puff method for enhanced oil recovery since the current oil recovery methods have a low recovery efficiency of about 10%. For this purpose, they used a microfluidic system to reveal

the mechanisms and to quantify the recovery rates of oil from fracture networks. The results showed that injection of supercritical CO_2 resulted in the highest recovery rate 90% and 60% while the recovery rates for N_2 were 40% and 25% in the connected and dead-end fracture networks respectively since N_2 has lower solubility in oil. In another study, a brine saturated microfluidic chip was used to investigate the effect of fluid viscosity, interfacial tension, injection rate

and the phase of CO₂ on the geological CO₂ sequestration (Zheng et al. 2017).

4 Supercritical microreactors: materials and fabrication methods

The main challenge for the combining of supercritical fluids and microfluidics is the design and fabrication of a system that can be operated successfully under process conditions especially elevated pressures. Several materials such as glass, metals, ceramics, polymers are available for the manufacturing of microfluidic systems. The material choice is highly dependent on the desired application conditions such as temperature, pressure, corrosivity of fluids, electrical and thermal properties and it has an impact on the selection of fabrication technique (Brandner 2013).

Rapid prototyping methods based on polymer molding are very popular as easy, fast and inexpensive fabrication techniques. Polydimethylsiloxane (PDMS) is the most commonly preferred polymer and used for the fabrication of transparent microchips which are suitable for the optical visualization and measurement techniques. However, PDMS

cannot be suitable for the production of microreactors for high pressure applications since it has poor temperature and pressure resistance (Martin et al. 2016; Ostmann and Kähler 2022). To reduce the channel deformation, a PDMS channel was sandwiched between two glass slides and the channel deformation was reported to be three times lower than the standard PDMS chips. Scientists also worked on the alternative polymers that are more pressure resistant than PDMS such as thermoset polyester (TPE), polyurethane methacrylate (PUMA) or Norland Adhesive 81 (NOA81). However, their pressure resistances were still low for the supercritical applications (Sollier et al. 2011). Martin et al. (2016) presented an inexpensive rapid prototyping method for the fabrication of microchannels made of UV-curable OSTEMER and glass to utilize with supercritical CO₂. The fabricated microchips were shown to resist high pressures up to 20 MPa for several hours and their transparency offered the possibility to observe and measure flow characteristics inside the microchannels (Fig. 4a).

Metals are most commonly used materials for conventional devices since they have chemical compatibility and thermal resistance. The main fabrication techniques for the metal microdevices are etching, micromachining and

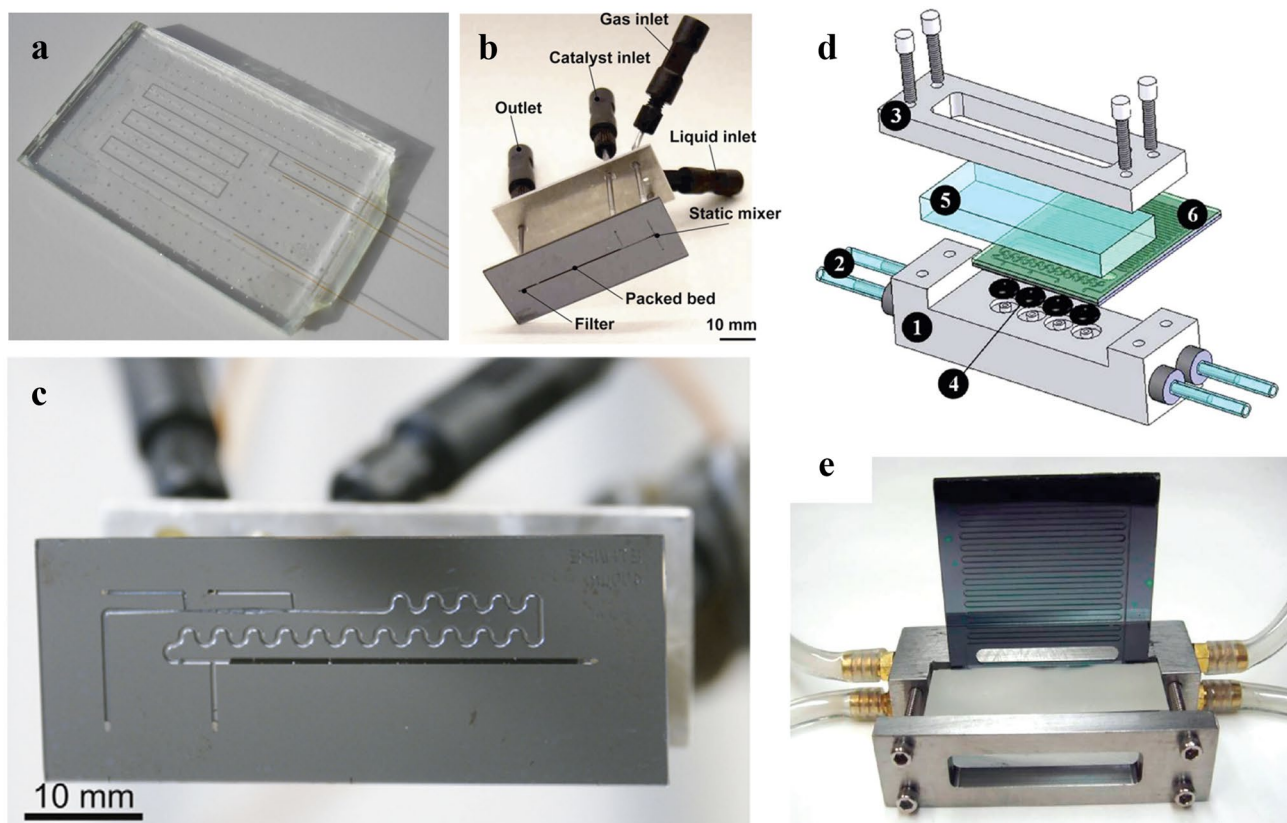


Fig. 4 Microreactors for high pressure applications. **a** OSTEMER microreactor, reproduced with permission (Martin et al. 2016) from Springer. **b, c** Si/glass microreactors, reproduced with permission

from (Trachsel et al. 2008, 2009) Elsevier. High pressure microsystem assembly. **d** scheme and **e** image, reproduced with permission (Marre et al. 2010) from ACS

selective laser melting. A stainless-steel microreactor was used for the gasification of glucose to hydrogen by supercritical water and it was shown that microreactors are promising tools to intensify the thermochemical conversion of biomass constituents to chemicals and fuels (Goodwin and Rorrer 2008). Yao et al. (2017) fabricated microchannels on stainless plates by chemical etching and using this microreactor, they studied the hydrodynamics and mass transfer of CO₂ absorption into water under elevated pressures. Ceramic microreactors are typically used for extremely high temperatures that are reachable neither with metals nor polymers. The steam reforming of propane was studied at temperatures between 800 and 1000 °C in ceramic microreactors and its potential for efficient on-site hydrogen production from hydrocarbons was reported (Christian and Kenis 2006). Despite its feasibility to high temperature applications, the interconnection between conventional equipments and ceramic devices is critical and special needs for sealing, assembling and joining have to be considered (Brandner 2013).

Glass is another popular material for the fabrication of microfluidic systems. It is chemically resistant against almost all chemicals and its optical transparency makes it a suitable material for applications which require optical visualization or measurements. Despite glass has high chemical resistance and structural stability, its tendency to fracture under tension makes it difficult to be structured. Silicon is another material which is also commonly used for the manufacturing of microsystems. Since the glass and silicon have similar mechanical properties, same fabrication techniques are used for both materials (Frank 2008; Han et al. 2021). Glass and silicon microreactors are manufactured by photolithographic techniques. In this technique, photolithographic glass plates coated with a thin metal and upper photoresist layers and desired channel network pattern is transferred from optical mask to the photoresist layer. At the next step, photoresist is exposed to light, developed and removed which is followed by etching and bonding processes (Watts and Haswell 2005). Trachsel et al. (2008) fabricated a Si/glass microreactor by a standard photolithography and dry etching technique and stainless steel capillaries were connected to microreactor by soldering (Fig. 4b). The system was mechanically tested by tensile and pressure tests and successfully applied for solid catalyzed exothermic hydrogenation at 5.1 MPa and 71 °C conditions. In the further study, they improved their design by adding a meandering mixing section (Fig. 4c) and used this microreactor for hydrogenation of cyclohexane by supercritical CO₂ (Trachsel et al. 2009). Tiggelaar et al. (2007) used a glass microreactor to study the formation of the carbamic acid by the reaction of N-benzylmethylamine and CO₂ under high pressure conditions and reported that the glass microreactor could be used for pressures up to 40 MPa without failure. In another study, a microfluidic device fabricated

by embedding the silicon capillaries in epoxy resin was suggested as transparent and inexpensive system for high pressure applications. They conducted experiments in an ionic liquid and supercritical CO₂ flow under isothermal conditions. The two-phase flow system was observed with a high-speed camera and operating pressures up to 30 MPa could be achieved in this system (Macedo Portela da Silva et al. 2014). Although the low thermal conductivity of glass limits its applications requiring good heat transfer, the high pressures can be reached using glass microreactors and they can be successfully used with supercritical CO₂ which has a low critical temperature value.

The connection of microfluidic systems to the macroscopic fluid handling systems is more challenging when working under supercritical conditions. Since the fluidic connections can be fabricated to fit the commercially available fittings, metal microreactors can be easily packed. For other microreactors, permanent integrated connections can be used to connect tubings. Marre et al. (2010) used a modular design consisting of two stainless steel parts with O-rings to compress the silicon/Pyrex microreactor (Fig. 4d, e).

5 Supercritical microfluidic applications of CO₂

5.1 Extraction

Supercritical CO₂ is a green alternative to organic solvents in biorefinery applications such as biomass pretreatment, extraction and chemical conversion and has been proven commercially for coffee decaffeination and hops extraction. It is a common knowledge that solvent properties of supercritical CO₂ such as polarity, density and viscosity can be easily tuned by small variations in temperature and pressure. While high density of CO₂ under supercritical conditions contributes to solubilisation of compounds, low viscosity enhances penetration into extraction matrix, thus challenging extraction processes can be easily conducted by supercritical CO₂. The low surface tension and absence of product contamination with solvent residues are other distinct advantages of supercritical CO₂ for extraction processes. In addition, properties such as electronic structure and charge separation affect the solvent properties of CO₂. For instance, CO₂ can act as a Lewis base or acid and participate in hydrogen bond interactions that lead the specific solute–solvent interaction and selective extraction of different compounds. Apart from solubility properties, external control and internal limitations for mass transfer significantly affect the rate of supercritical CO₂ extraction. Supercritical extraction processes mainly focus on extract yield which is not only dependent on temperature and pressure conditions but also physical characteristics of extraction matrix such

porosity, density and geometry of bed, particle size and particle size distribution (Weibel and Ober 2003; Sahena et al. 2009; Huang et al. 2012; Kazan et al. 2014; Zhu et al. 2018; Kwan et al. 2018). Integration of supercritical extraction in microfluidic systems has drawn attention with the advantages of precise control and accelerated extraction properties. However, the main disadvantage of these systems is the separation since surface forces dominates over body forces in micro scale and separation by gravity cannot be applied.

Continuous extraction of vanillin, an important flavoring agent, was carried out by segmented flow of supercritical CO₂ in a silicon/glass microextractor which was integrated with a capillary separation device (Fig. 5a, b). The system operated under 8–11 MPa and equilibrium was reached after pretty short time (1.6–2.8 s) with highly reproducible equilibrium concentrations (Assmann et al. 2012). Cheng et al. (2018) performed supercritical CO₂ extraction of astaxanthin from *Haematococcus pluvialis* in a microfluidic reactor. A hydrothermal cell disruption step was added before the extraction since the direct extraction of wet microalgae biomass using supercritical CO₂ is generally not feasible as a result of the rigid cell wall. First, the cells were loaded into the microfluidic reactor and hydrothermal disruption of the cells was carried out at 200 °C and 8 MPa for 10 min that provided uniform and thorough disruption to all cells. Then, supercritical CO₂ extraction was carried out on disrupted cells with pure or co-solvent added CO₂ and a dark-field microscope was used to observe the cells and the color change. The timescales of extraction process at 55 °C were reduced 1800-fold from 15 h to 30 s by the addition of

ethanol as a co-solvent while the extraction was completed in 180 s for the using of olive oil as a co-solvent instead of ethanol. Assmann et al. (2013) used a continuous flow microfluidic device for direct extraction of lignin oxidation products such as vanillin, methyl vanillate and 5-carbomethoxy-vanillin from aqueous reaction mixture using supercritical CO₂ as a solvent. Higher quantities of monomers were extracted with increasing pressure and decreasing temperature with high selectivity. The results showed that different selectivity of supercritical CO₂ towards lignin oxidation products makes it a suitable solvent for separation and enables the use of this method to remove methyl 5-carbomethoxy-vanillate and concentrate vanillin and methyl vanillate in the raffinate phase.

Supercritical fluids are also used for the extraction of metal complexes from solid and aqueous media as an alternative to traditional solvent extraction methods. Ohashi et al. (2011) developed a microfluidic system to measure the distribution of tris(acetylacetonato)-cobalt(III) (Co(acac)₃) between supercritical CO₂ and water. A glass microchip with and without modification by dichlorodimethylsilane was used and modification was shown to induce phase separation of CO₂ and water inside microchannel and the (Co(acac)₃) concentration in aqueous phase increased by the increasing the contact time of two phases.

5.2 Reactions in microreactor with supercritical CO₂

Compared to the batch systems, continuously operated microfluidic systems allow the fast screening of reaction

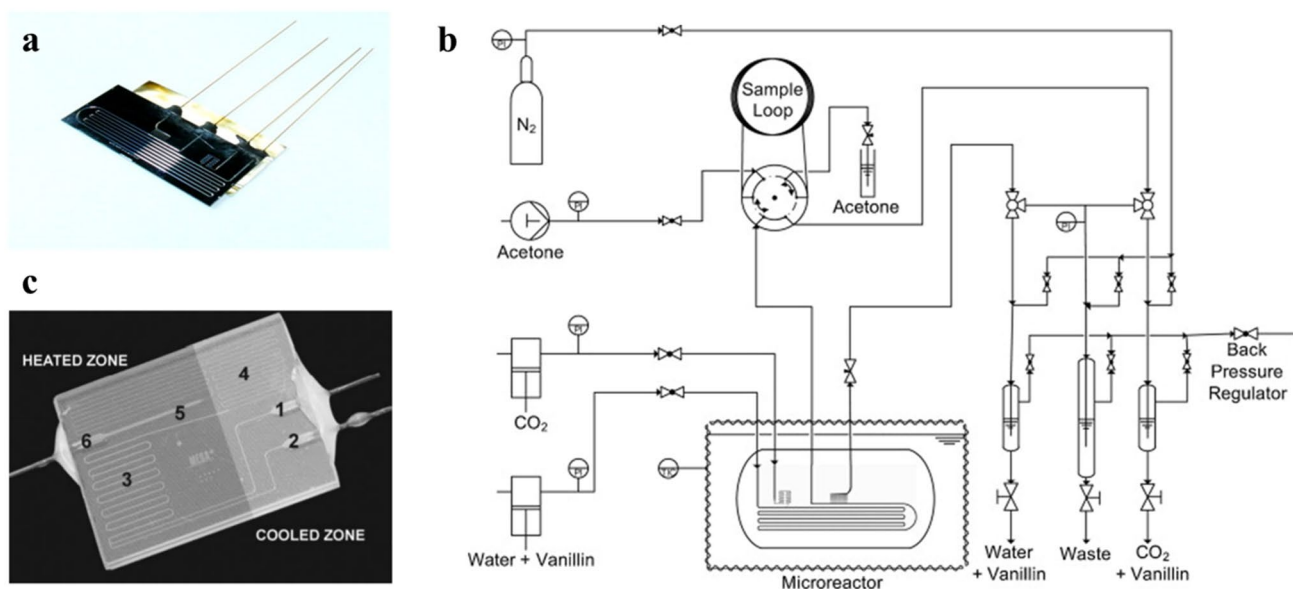


Fig. 5 **a** Silicon/glass microdevice and **b** scheme of the high pressure plant for vanillin extraction, reproduced with permission from (Assmann et al. 2012) Elsevier. **c** Photograph of a microreactor for

phthalic anhydride esterification, reproduced with permission from (Benito-Lopez et al. 2007) RSC

conditions, consume small amount of reagents and due to the small volumes, minimize the risk that may arise from elevated pressure and temperature under supercritical conditions (Assmann et al. 2013; Kazan et al. 2017). Enhanced heat and mass transfer properties lead to effective control of reaction conditions and make the microfluidic systems more advantageous to carry out highly exothermic reactions.

The variations in temperature and pressure affect some properties of supercritical CO₂ such as viscosity, density and dielectric constant and result in changes in reaction yields, kinetics and selectivity. Benito-Lopez et al. (2007) described a glass microreactor and studied the effects of pressure and supercritical CO₂ on the reaction rate of phthalic anhydride esterification (Fig. 5c). It was shown that the use of a microreactor for the esterification reaction enhanced the reaction rate constant even at low pressures (1.6×10^{-3} and $3.1 \times 10^{-3} \text{ M}^{-1} \text{ s}^{-1}$ at 9 and 11 MPa, respectively) and the ratio of microreactor and batch reaction rate constants increased with increasing temperature. Compared to conventional reaction systems, microreactors operated in continuous flow mode with pressure showed to significantly enhance the reaction rate. In another study, supercritical CO₂ was used as a solvent for the esterification of oleic acid with methanol in a microfluidic device. Results showed that esterification reaction occurred in less than 1 min even without any catalyst and addition of small amount of catalyst increased the yield fourfold and rate constant of uncatalyzed and catalyzed reactions were calculated as 0.0036 and 0.0634 s^{-1} , respectively (Quitain et al. 2018).

Hydrogenation reactions are a class of reactions which are important for pharmaceutical and chemical industries. The low interaction efficiency and mass transfer between different phases result in slow reaction rates. Since the transfer rate of hydrogen from gas phase to liquid phase is critical for the reaction rate, it is important to overcome both heat and mass transfer limitations between two phases. Although the addition of equipment for a higher interfacial area, variation of stirring speed or particle size are commonly used to enhance the mass transfer, these approaches have still limitations. In addition, transport limitations were shown to affect the product distribution for the hydrogenation of fatty oils over Ni catalyst. Therefore, development of new systems with higher interfacial area becomes important to enhance the mass and heat transfer between two phases (Singh and Vannice 2001; Kobayashi et al. 2004). With large interfacial area and effective heat and mass transfer properties, microfluidics can be used as an alternative system for the hydrogenation reactions. Although the mechanism is not clear, solvent type also affects the reaction rate and product distribution probably by the solvent polarity or dielectric constant. While supercritical CO₂ has liquid-like properties that allow the dissolution of several organic compounds, its gas-like properties make it highly miscible in other gases such as

hydrogen. The combination of supercritical CO₂ and microfluidics create a suitable system for high performance hydrogenation reactions. A Pd-immobilized microchannel reactor was prepared for the hydrogenation reaction in supercritical CO₂ and a variety of substrates were used and converted to desired products successfully. The reaction time was less than a second and using of supercritical CO₂ as a solvent both increased the solubility of hydrogen and productivity (0.1 mmol h^{-1} per channel) compared to the experiments using tetrahydrofuran as a solvent (0.01 mmol h^{-1} per channel) (Kobayashi et al. 2005). In another study, a packed bed Si/glass microreactor fabricated by photolithography was used for the hydrogenation of cyclohexene and supercritical CO₂ was used as reaction solvent. The microfluidic systems contained three inlets: cyclohexene and H₂ were pumped through separate inlets to generate a segmented gas–liquid flow and supercritical CO₂ was pumped through the third inlet to dissolve the cyclohexene–H₂ mixture. To obtain a single phase reaction mixture, a meandering mixing channel was added to microreactor design which was followed by a packed bed channel containing catalyst particles. Molar ratio of CO₂:cyclohexene:H₂ kept constant at 90:5:5, temperature and pressure were varied to determine the effect of operating conditions on reaction performance. An increase about fivefold in reaction rate with increasing temperature from 40 to 70 °C was observed while pressure showed no significant effect on reaction rate. Performances of different reactor systems were compared in terms of space time yield ($\text{kg}_{\text{product}}/\text{hm}^3_{\text{catalyst}}$) and the space time yield was one order of magnitude greater than larger scale systems. The results indicated that high pressure microreactor system was suitable for exothermic reactions as a result of effective heat removal characteristic (Trachsel et al. 2009). Urakawa et al. (2008) combined this system with Raman spectroscopy to fast and simultaneous analysis of product concentration profile of cyclohexene hydrogenation in supercritical CO₂. After mixing in meandering channel, the Raman spectrum showed only the characteristic bands of cyclohexene, while the product, cyclohexane, band gradually increased as the mixture flowed through the packed catalyst bed and the final conversion could be monitored at the outlet channel. Table 2 summarizes high pressure reactions in microfluidic systems.

5.3 Synthesis of micro and nano sized materials in microfluidics

In microfluidic systems, fluids can flow in single-phase or multi-phase state for miscible and immiscible fluids, respectively. For immiscible fluids, fluids can be either co-flow or discontinuous flow of one fluid as droplets in the continuous flow of other fluid which is called as droplet microfluidics. Droplet microfluidics can also be applied to

Table 2 High pressure reactions in microfluidic systems

Microreactor	Reaction	Conditions	Catalyst	Reaction time	Main result	Reference
Glass microreactor	Esterification of phthalic anhydride with methanol	20–100 °C 9 and 11 MPa	–	–	Reaction rate enhancement	Benito-Lopez et al. (2007)
Stainless steel microreactor	Esterification of oleic acid with methanol	60–100 °C 10 MPa	H ₂ SO ₄	< 1 min	fourfold increase in reaction yield	Quitain et al. (2018)
Pd-immobilized glass microreactor	Hydrogenation of different substrates	60 °C 9 MPa	Pd	1 s	High reaction productivity	Kobayashi et al. (2005)
Packed bed Si/glass microreactor	Hydrogenation of cyclohexene	40–70 °C 8–15 MPa	Pd/Al ₂ O ₃	–	Larger space time yield	Trachsel et al. (2009)
Packed bed Si/glass microreactor	Hydrogenation of cyclohexene	305–318 K 10 MPa	Pd/Al ₂ O ₃	–	Potential of on-chip Raman analysis	Urakawa et al., 2008

gas–liquid systems where the droplets were replaced with gas bubbles (Abolhasani et al. 2014).

Microbubbles, which consist of a shell and gas core, are theranostic agents that provide contrast for imaging (diagnostic) and drug delivery for targeted therapy simultaneously. The diameter of a microbubble is less than 10 µm which is equal to the size of a red blood cell. Since the bubbles at this size are unstable in aqueous media, surfactants, lipids, proteins and polymers are used separately or in combination to stabilize the shell structure. Microbubbles resonate by the sound wave of the ultrasound equipment and create a high contrast as a result of the different acoustic response of resonating microbubbles and surrounding tissue. The size of each microbubble is important and should be in a narrow range to obtain information with high efficiency. Although their properties have to be tailored to strict specifications in medical applications, conventional microbubble preparation methods like sonication or layer-by-layer biopolymer deposition are insufficient to produce bubbles with controlled size. On the other hand, microfluidic systems provide an environment with a precise control for the microbubble formation (Ahmad et al. 2008; Yang et al. 2009; Sirsi and Borden 2009; Enayati et al. 2011). Tumarkin et al. (2011) used a microfluidic device to produce highly monodisperse particle-coated microbubbles and the response of CO₂ bubbles to the temperature variation was examined. They showed that the size of CO₂ bubbles decreased by lowering temperature as a result of enhanced CO₂ dissolution in water at reduced temperatures. In another study, an aqueous NaOH solution containing poly(styrene-co-acrylic acid) nanoparticles and gaseous CO₂ were fed to a microfluidic device with a T-junction to produce plugs of CO₂. Stable armored bubbles were obtained with a narrow size distribution (polydispersity of 2–5%) and method productivity was increased from 700 bubbles/s to 3000 bubbles/s by a microfluidic flow-focusing bubble generator (Park et al. 2009).

Supercritical fluids are used for the preparation of micro- and nanoparticles for many years and supercritical CO₂ is one of the most attractive solvent due to its mild processing conditions. Mixing is the one of the most important parameter during particle synthesis and has a significant impact on particle size and size distribution. Since microsystems provide a strict control on synthesis conditions and enhanced mixing performance, supercritical microfluidics are more advantageous over conventional particle preparation approaches to produce particles with uniform size distribution in a narrow range. A high pressure silicon-Pyrex microreactor was designed for the preparation of poly-(3-hexylthiophene) (P3HT) nanoparticles by supercritical antisolvent (SAS) process (Fig. 6a). The system was operated under 40–50 °C temperature and 8–10 MPa pressure ranges. CO₂ was fed to system and after it reached the desired temperature and pressure values, P3HT solution was fed through the mixing point creating a full 3D coaxial injection. A jet was formed between the CO₂ and P3HT solution at the mixing point and quickly disappeared upon fast mixing leading to nanoparticle nucleation with an average size of 36 nm (Couto et al. 2015). Jaouhari et al. (2020) combined supercritical antisolvent (SAS) process and microfluidic systems to improve the control, performance and the reproducibility of the operation. Tetrahydrofuran (THF) was used as the solvent while supercritical CO₂ was antisolvent and tetraphenylethylene (TPE) nanoparticles were synthesized in a homemade silicon-Pyrex microchip under 40 °C and 10 MPa. Obtained nanoparticles were analyzed with transmission electron microscope and specified by having particle sizes below 15 nm. Results also showed that the variation of experimental parameters such as initial TPE concentration and flow rates strongly affect the hydrodynamics of mixing process and mean particle size.

Jaouhari et al. (2022) fabricated a Pyrex/silicon microfluidic device by photolithography/wet etching/anodic bonding protocol. The device was used as a micromixer and operated under 40 °C and 10 MPa to analyze mixing, nucleation and

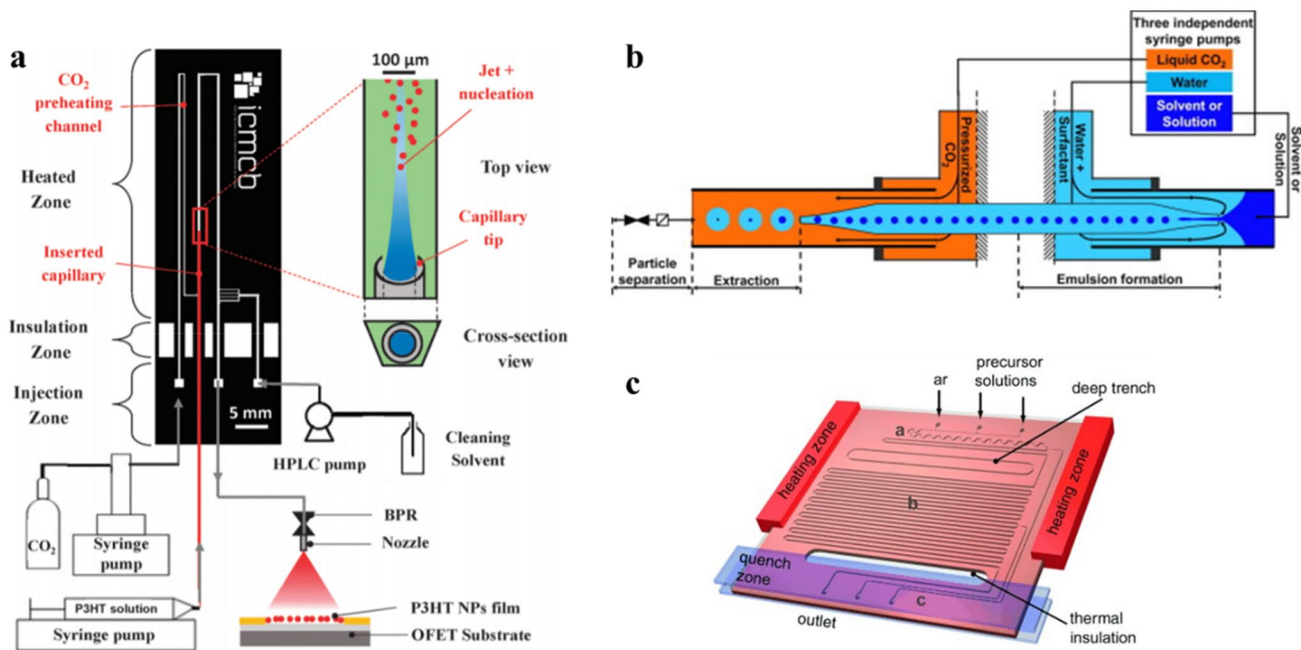


Fig. 6 **a** Microsystem for P3HT nanoparticle synthesis, reproduced with permission from (Couto et al. 2015) RSC. **b** Micro-capillary system for emulsion extraction, reproduced with permission from

(Luther and Braeuer 2012) Elsevier. **c** Microreactor for quantum dot synthesis, reproduced with permission from (Yen et al. 2005) Wiley

growth characteristics in THF/scCO₂ system. A fluorescent organic dye molecule was used for in situ visualization and particles with a mean size of 16 nm were successfully prepared.

Extraction of emulsions is another application of supercritical CO₂ for the production of nanoparticles. For instance, cholesterol acetate, griseofulvin and megestrol acetate nanoparticles were produced by extraction of oil-in-water emulsions using supercritical carbon dioxide (Shekunov et al. 2006). Ajiboye et al. (2018) produced polycaprolactone (PCL) nanoparticles via supercritical fluid extraction of emulsions using supercritical CO₂ and spherical nanoparticles with mean particle sizes between 190 and 350 nm were obtained depending on the polymer concentration. Recently, microfluidic devices have been used for the emulsion extraction under high pressure conditions. In this approach, supercritical CO₂ was used to rapidly extract the solvent or oil phase of an emulsion that leads the precipitation of solute and results in an aqueous suspension containing nanoparticles. Luther and Braeuer (2012) used a microfluidic device consisting of thin fused silica capillaries to investigate the ethyl acetate–water–supercritical CO₂ solvent system for the particle formation by supercritical fluid extraction of emulsions method (Fig. 6b). They reported that properties of microfluidic systems provided homogenous conditions, fast process control and detection and production of mono-disperse emulsion. In another work, supercritical CO₂ was applied to a microfluidic system with a T-junction for the

extraction of polyvinyl alcohol nanoparticles from ethyl acetate-water emulsion and slug-flow patterns were captured by a camera. No residual ethyl acetate was observed in the suspension that indicated the successful extraction of the ethyl acetate in emulsion by supercritical CO₂ and authors pointed their expectation for the reduction of cost and operation time for the production of nanoparticle suspensions in a microfluidic slug-flow system using supercritical CO₂ (Murakami and Shimoyama 2016). Ibuprofen nanosuspension was fabricated by supercritical fluid extraction of emulsion in a microfluidic system and prepared nanoparticles were functionalized by chitosan. Authors showed that the size of particles in the suspension could be controlled by the amount of ibuprofen loaded in ethyl acetate droplets in ethyl acetate/water emulsion (Murakami and Shimoyama 2017). The effect of supercritical carbon dioxide on the formation and stability of water-in-oil emulsions was investigated under high pressure conditions. For this purpose, a Y-junction made of PMMA was designed and operated at pressures from 0.1 to 15 MPa with by monitoring with a high-speed camera. It was reported that larger droplets and thicker jets were produced with increasing pressure as a result of low capillary numbers and high Weber numbers (Jaouhari et al. 2020).

Nanometer-sized colloidal crystals, nanocrystals, have various applications in optoelectronics, catalyst and nanomedicine. For a successful application, properties of nanocrystals such as well-defined size, shape, composition

and crystallinity are important in all application fields. The main problem of the conventional production methods is the difference in product quality between batches. For improved product control, the better uniformity in thermal and chemical environment can be obtained using microfluidic systems (Phillips et al. 2014). The first microfabricated gas–liquid segmented flow for high temperature nanocrystal synthesis was reported by Yen et al. (2005) (Fig. 6c). They prepared CdSe quantum dots from cadmium 2,4-pentanedionate and selenium at 260 °C. They showed that good size control could be achieved by tuning the injection rates of the cadmium and selenium precursor solutions and significantly narrower emission spectra than an equivalent single-phase synthesis was reported. The advantage of using a supercritical fluid for the nanocrystal synthesis was demonstrated in a study in which a high pressure high temperature microreactor and supercritical hexane was used for CdSe quantum dot synthesis (Marre et al. 2008). Size distribution of quantum dots synthesized in supercritical hexane and in liquid phase was 4–6% and 9–12%, respectively that showed the advantage of microfluidic system with narrower residence time distribution and more homogenous reaction conditions. In another study, exciton luminescent ZnO nanocrystals were synthesized using continuous supercritical microfluidics and

obtained ZnO nanocrystals with a better control in size and shape (Roig et al. 2011). Palladium nanocrystals were synthesized in a co-flow capillary microsystem by the hydrogen reduction of palladium (II) precursors in the presence of organic stabilizers. Since the hydrogen is poorly soluble in toluene, a commonly used solvent, supercritical CO₂ was added to toluene to enhance the hydrogen solubility. Catalytic activity of nanocrystals is highly dependent on surface properties and co-axial flow was shown to allow precise construction of the catalyst architectures, as intended for a targeted reaction (Gendrineau et al. 2012). Table 3 summarizes micro and nano-sized material synthesis in microfluidic systems.

6 Conclusions

This paper presents a short overview of the supercritical CO₂ applications in microfluidic systems. Although the critical point of a substance was discovered in early nineteenth century, first applications of supercritical fluids were started in mid 1900s and gained a huge attention over the last decades. As a newly developed field, supercritical microfluidics has a great advantage by combining the properties of supercritical

Table 3 Micro and nano sized material synthesis in microfluidics

Microreactor	Application	Conditions	Main result	Reference
PDMS	Production of particle encapsulated CO ₂ bubbles	1–70 °C	Controlling the CO ₂ dissolution by changing temperature Highly monodisperse bubble formation	Tumarkin et al. (2011)
PDMS microfluidic T-junction device	Production of particle encapsulated CO ₂ bubbles	28 °C	Increased productivity from 700 bubbles/s to 3000 bubbles/s Controlled bubble size	Park et al. (2009)
Silicon/pyrex microreactor	Synthesis of semiconducting nanoparticles by microfluidic SAS process	40–50 °C 8–10 MPa	Production of nanoparticles with an average diameter of 36 nm	Couto et al. (2015)
Fused silica capillaries	Supercritical fluid extraction of emulsion by CO ₂	311 K 8.5 MPa	Homogenous conditions Fast process control and detection Production of monodisperse emulsion	Luther and Braeuer (2012)
Polyphenyl sulfone microcapillary tube	Extraction of polyvinyl alcohol (PVA) nanoparticles by CO ₂	313 K 8–10 MPa	Particle size reduction Successful extraction of organic solvent from suspension	Murakami and Shimoyama (2016)
Polyphenyl sulfone microchannel	Extraction of PVA nanoparticles by CO ₂ and functionalization with chitosan	310 K 10 MPa	Controlled particle size Narrow size distribution 140 times higher drug loading	Murakami and Shimoyama (2017)
Silicon/pyrex microreactor	Synthesis of quantum dots by supercritical hexane	270 °C 5 MPa	Safer high pressure process Better reproducibility Narrow size distribution	Marre et al. (2008)
Fused silica capillaries	Synthesis of luminescent ZnO nanocrystals	250 °C 25 MPa	Better control in size and shape	Roig et al. (2011)
Capillary microsystem	Synthesis of palladium nanocrystals	100 °C 25 MPa	Precise construction of nanocrystal architectures	Gendrineau et al. (2012)

fluids and microfluidics and already proved its potential with highly efficient and selective extraction processes, improved reaction conditions and strict control of particle formation. It is expected that the interest in supercritical microfluidics will continue to increase and advances in high pressure technologies and microfabrication techniques will open up new pathways for novel applications.

Declarations

Conflict of interest The author has no relevant financial or non-financial interests to disclose.

References

- Abolhasani M, Günther A, Kumacheva E (2014) Microfluidic studies of carbon dioxide. *Angew Chem Int Ed* 53:7992–8002. <https://doi.org/10.1002/anie.201403719>
- Adami R, Schuster J, Liparoti S et al (2013) A Raman spectroscopic method for the determination of high pressure vapour liquid equilibria. *Fluid Phase Equilib* 360:265–273. <https://doi.org/10.1016/J.FLUID.2013.09.046>
- Ahmad Z, Zhang HB, Farook U et al (2008) Generation of multilayered structures for biomedical applications using a novel tri-needle coaxial device and electrohydrodynamic flow. *J R Soc Interface* 5:1255–1261. <https://doi.org/10.1098/rsif.2008.0247>
- Ajiboye AL, Trivedi V, Mitchell JC (2018) Preparation of polycaprolactone nanoparticles via supercritical carbon dioxide extraction of emulsions. *Drug Deliv Transl Res* 8:1790–1796. <https://doi.org/10.1007/s13346-017-0422-3>
- Antes J, Boskovic D, Krause H et al (2003) Analysis and improvement of strong exothermic nitrations in microreactors. *Chem Eng Res Des* 81:760–765. <https://doi.org/10.1205/026387603322302931>
- Assmann N, Kaiser S, Rudolf von Rohr P (2012) Supercritical extraction of vanillin in a microfluidic device. *J Supercrit Fluids* 67:149–154. <https://doi.org/10.1016/J.SUPFLU.2012.03.015>
- Assmann N, Werhan H, Ładosz A, Rudolf von Rohr P (2013) Supercritical extraction of lignin oxidation products in a microfluidic device. *Chem Eng Sci* 99:177–183. <https://doi.org/10.1016/j.ces.2013.05.032>
- Benito-Lopez F, Tiggelaar RM, Salbut K et al (2007) Substantial rate enhancements of the esterification reaction of phthalic anhydride with methanol at high pressure and using supercritical CO₂ as a co-solvent in a glass microreactor. *Lab Chip* 7:1345–1351. <https://doi.org/10.1039/b703394j>
- Blanchard LA, Brennecke JF (2001) Recovery of organic products from ionic liquids using supercritical carbon dioxide. *Ind Eng Chem Res* 40:287–292. <https://doi.org/10.1021/ie000710d>
- Blanch-Ojea R, Tiggelaar RM, Pallares J et al (2012) Flow of CO₂-ethanol and of CO₂-methanol in a non-adiabatic microfluidic T-junction at high pressures. *Microfluid Nanofluidics* 12:927–940. <https://doi.org/10.1007/s10404-011-0927-x>
- Boock JT, Freedman AJE, Tompsett GA et al (2019) Engineered microbial biofuel production and recovery under supercritical carbon dioxide. *Nat Commun* 10:587. <https://doi.org/10.1038/s41467-019-08486-6>
- Brandner JJ (2013) Fabrication of microreactors made from metals and ceramic. *Microreactors Org Chem Catal Second Ed*. <https://doi.org/10.1002/9783527659722.ch2>
- Brown ZK, Fryer PJ, Norton IT, Bridson RH (2010) Drying of agar gels using supercritical carbon dioxide. *J Supercrit Fluids* 54:89–95. <https://doi.org/10.1016/j.supflu.2010.03.008>
- Cheng X, Qi Z, Burdyny T et al (2018) Low pressure supercritical CO₂ extraction of astaxanthin from *Haematococcus pluvialis* demonstrated on a microfluidic chip. *Bioresour Technol* 250:481–485. <https://doi.org/10.1016/J.BIORTECH.2017.11.070>
- Christian MM, Kenis PJA (2006) Ceramic microreactors for on-site hydrogen production from high temperature steam reforming of propane. *Lab Chip* 6:1328–1337. <https://doi.org/10.1039/B607552E>
- Ciceri D, Perera JM, Stevens GW (2014) The use of microfluidic devices in solvent extraction. *J Chem Technol Biotechnol* 89:771–786. <https://doi.org/10.1002/jctb.4318>
- Couto R, Chambon S, Aymonier C et al (2015) Microfluidic supercritical antisolvent continuous processing and direct spray-coating of poly(3-hexylthiophene) nanoparticles for OFET devices. *Chem Commun* 51:1008–1011. <https://doi.org/10.1039/C4CC07878K>
- Coyle EE, Oelgemöller M (2008) Micro-photochemistry: photochemistry in microstructured reactors. The new photochemistry of the future? *Photochem Photobiol Sci* 7:1313–1322. <https://doi.org/10.1039/B808778D>
- Deleau T, Letourneau JJ, Camy S et al (2022) Determination of mass transfer coefficients in high-pressure CO₂-H₂O flows in microcapillaries using a colorimetric method. *Chem Eng Sci* 248:117161. <https://doi.org/10.1016/J.CES.2021.117161>
- Elvira KS, Solvas XC, Wootton RCR, deMello AJ (2013) The past, present and potential for microfluidic reactor technology in chemical synthesis. *Nat Chem* 5:905
- Enayati M, Chang M-W, Bragman F et al (2011) Electrohydrodynamic preparation of particles, capsules and bubbles for biomedical engineering applications. *Colloids Surf A Physicochem Eng Asp* 382:154–164. <https://doi.org/10.1016/J.COLSURFA.2010.11.038>
- Frank T (2008) Fabrication and assembling of microreactors made from glass and silicon. *Microreactors Org Synth Catal*. <https://doi.org/10.1002/9783527622856.ch2>
- Gendrineau T, Marre S, Vaultier M et al (2012) Microfluidic synthesis of palladium nanocrystals assisted by supercritical CO₂: tailored surface properties for applications in boron chemistry. *Angew Chemie* 124:8653–8656. <https://doi.org/10.1002/ange.201203083>
- Goodwin AK, Rorrer GL (2008) Conversion of glucose to hydrogen-rich gas by supercritical water in a microchannel reactor. *Ind Eng Chem Res* 47:4106–4114. <https://doi.org/10.1021/ie701725p>
- Guillaumont R, Erriguible A, Aymonier C et al (2013) Numerical simulation of dripping and jetting in supercritical fluids/liquid micro coflows. *J Supercrit Fluids* 81:15–22. <https://doi.org/10.1016/J.SUPFLU.2013.04.011>
- Günther A, Jensen KF (2006) Multiphase microfluidics: from flow characteristics to chemical and materials synthesis. *Lab Chip* 6:1487–1503. <https://doi.org/10.1039/B609851G>
- Gurikov P, Raman SP, Weinrich D et al (2015) A novel approach to alginate aerogels: carbon dioxide induced gelation. *RSC Adv* 5:7812–7818. <https://doi.org/10.1039/C4RA14653K>
- Han Y, Jiao Z, Zhao J et al (2021) A simple approach to fabricate multi-layer glass microfluidic chips based on laser processing and thermocompression bonding. *Microfluid Nanofluidics* 25:77. <https://doi.org/10.1007/s10404-021-02479-y>
- Ho T-HM, Yang J, Tsai PA (2021a) Microfluidic mass transfer of CO₂ at elevated pressures: implications for carbon storage in deep saline aquifers. *Lab Chip* 21:3942–3951. <https://doi.org/10.1039/D1LC00106J>
- Ho THM, Sameoto D, Tsai PA (2021b) Multiphase CO₂ dispersions in microfluidics: formation, phases, and mass transfer. *Chem*

- Eng Res Des 174:116–126. <https://doi.org/10.1016/J.CHERD.2021.07.006>
- Hu J, Deng W (2016) Application of supercritical carbon dioxide for leather processing. *J Clean Prod* 113:931–946. <https://doi.org/10.1016/j.jclepro.2015.10.104>
- Huang Z, Shi X, Han, Jiang W Juan, (2012) Theoretical models for supercritical fluid extraction. *J Chromatogr A* 1250:2–26. <https://doi.org/10.1016/J.CHROMA.2012.04.032>
- Janicke MT, Kestenbaum H, Hagedorf U et al (2000) The controlled oxidation of hydrogen from an explosive mixture of gases using a microstructured reactor/heat exchanger and Pt/Al₂O₃ catalyst. *J Catal* 191:282–293. <https://doi.org/10.1006/jcat.2000.2819>
- Jaouhari T, Zhang F, Tassaing T et al (2020) Process intensification for the synthesis of ultra-small organic nanoparticles with supercritical CO₂ in a microfluidic system. *Chem Eng J* 397:125333. <https://doi.org/10.1016/j.cej.2020.125333>
- Jaouhari T, Marre S, Tassaing T et al (2022) Investigating nucleation and growth phenomena in microfluidic supercritical antisolvent process by coupling in situ fluorescence spectroscopy and direct numerical simulation. *Chem Eng Sci* 248:117240. <https://doi.org/10.1016/J.CES.2021.117240>
- Karimi R, Rezazadeh S, Raad M (2021) Investigation of different geometrical configurations effect on mixing performance of passive split-and-recombine micromixer. *Microfluid Nanofluidics* 25:90. <https://doi.org/10.1007/s10404-021-02491-2>
- Kazan A, Koyu H, Turu IC, Yesil-Celiktas O (2014) Supercritical fluid extraction of *Prunus persica* leaves and utilization possibilities as a source of phenolic compounds. *J Supercrit Fluids* 92:55–59. <https://doi.org/10.1016/J.SUPFLU.2014.05.006>
- Kazan A, Heymuth M, Karabulut D et al (2017) Formulation of organic and inorganic hydrogel matrices for immobilization of β-glucosidase in microfluidic platform. *Eng Life Sci* 17:714–722. <https://doi.org/10.1002/elsc.201600218>
- Knaust S, Andersson M, Hjort K, Klintberg L (2016) Influence of surface modifications and channel structure for microflows of supercritical carbon dioxide and water. *J Supercrit Fluids* 107:649–656. <https://doi.org/10.1016/J.SUPFLU.2015.07.027>
- Knittel D, Saus W, Schollmeyer E (1993) Application of supercritical carbon dioxide in finishing processes. *J Text Inst* 84:534–552. <https://doi.org/10.1080/00405009308658986>
- Kobayashi J, Mori Y, Okamoto K et al (2004) A microfluidic device for conducting gas–liquid–solid hydrogenation reactions. *Science* 304:1305–1308. <https://doi.org/10.1126/science.1096956>
- Kobayashi J, Mori Y, Kobayashi S (2005) Hydrogenation reactions using scCO₂ as a solvent in microchannel reactors. *Chem Commun*. <https://doi.org/10.1039/B501169H>
- Krühne U, Heintz S, Ringborg R et al (2014) Biocatalytic process development using microfluidic miniaturized systems. *Green Process Synth* 3:23–31. <https://doi.org/10.1515/gps-2013-0089>
- Kumari R, Dutta PK (2010) Physicochemical and biological activity study of genipin-crosslinked chitosan scaffolds prepared by using supercritical carbon dioxide for tissue engineering applications. *Int J Biol Macromol* 46:261–266. <https://doi.org/10.1016/j.ijbmac.2009.12.009>
- Kwan TA, Kwan SE, Peccia J, Zimmerman JB (2018) Selectively biorefining astaxanthin and triacylglycerol co-products from microalgae with supercritical carbon dioxide extraction. *Bioreour Technol* 269:81–88. <https://doi.org/10.1016/J.BIORTECH.2018.08.081>
- Leitner W (2002) Supercritical carbon dioxide as a green reaction medium for catalysis. *Acc Chem Res* 35:746–756. <https://doi.org/10.1021/ar010070q>
- Liu J, Hansen C, Quake SR (2003) Solving the “world-to-chip” interface problem with a microfluidic matrix. *Anal Chem* 75:4718–4723. <https://doi.org/10.1021/ac0346407>
- Luther SK, Braeuer A (2012) High-pressure microfluidics for the investigation into multi-phase systems using the supercritical fluid extraction of emulsions (SFEE). *J Supercrit Fluids* 65:78–86. <https://doi.org/10.1016/J.SUPFLU.2012.02.029>
- Luther SK, Stehle S, Weihs K et al (2015) Determination of vapor-liquid equilibrium data in microfluidic segmented flows at elevated pressures using Raman spectroscopy. *Anal Chem* 87:8165–8172. <https://doi.org/10.1021/acs.analchem.5b00699>
- Macedo Portela da Silva N, Letourneau J-J, Espitalier F, Prat L (2014) Transparent and inexpensive microfluidic device for two-phase flow systems with high-pressure performance. *Chem Eng Technol* 37:1929–1937. <https://doi.org/10.1002/ceat.201400028>
- Marre S, Jensen KF (2010) Synthesis of micro and nanostructures in microfluidic systems. *Chem Soc Rev* 39:1183–1202. <https://doi.org/10.1039/b821324k>
- Marre S, Park J, Rempel J et al (2008) Supercritical continuous-microflow synthesis of narrow size distribution quantum dots. *Adv Mater* 20:4830–4834. <https://doi.org/10.1002/adma.200801579>
- Marre S, Adamo A, Basak S et al (2010) Design and packaging of microreactors for high pressure and high temperature applications. *Ind Eng Chem Res* 49:11310–11320. <https://doi.org/10.1021/ie101346u>
- Martin A, Teychené S, Camy S, Aubin J (2016) Fast and inexpensive method for the fabrication of transparent pressure-resistant microfluidic chips. *Microfluid Nanofluidics* 20:92. <https://doi.org/10.1007/s10404-016-1757-7>
- Martin A, Camy S, Aubin J (2018) Hydrodynamics of CO₂-ethanol flow in a microchannel under elevated pressure. *Chem Eng Sci* 178:297–311. <https://doi.org/10.1016/J.CES.2017.12.046>
- Mendes RL, Nobre BP, Cardoso MT et al (2003) Supercritical carbon dioxide extraction of compounds with pharmaceutical importance from microalgae. *Inorg Chim Acta* 356:328–334. [https://doi.org/10.1016/S0020-1693\(03\)00363-3](https://doi.org/10.1016/S0020-1693(03)00363-3)
- Morini GL, Lorenzini M, Salvigni S, Spiga M (2009) Analysis of laminar-to-turbulent transition for isothermal gas flows in microchannels. *Microfluid Nanofluidics* 7:181–190. <https://doi.org/10.1007/s10404-008-0369-2>
- Mou J, Ren Y, Wang J et al (2022) Nickel oxide nanoparticle synthesis and photocatalytic applications: evolution from conventional methods to novel microfluidic approaches. *Microfluid Nanofluidics* 26:25. <https://doi.org/10.1007/s10404-022-02534-2>
- Murakami Y, Shimoyama Y (2016) Supercritical extraction of emulsion in microfluidic slug-flow for production of nanoparticle suspension in aqueous solution. *J Supercrit Fluids* 118:178–184. <https://doi.org/10.1016/J.SUPFLU.2016.08.009>
- Murakami Y, Shimoyama Y (2017) Production of nanosuspension functionalized by chitosan using supercritical fluid extraction of emulsion. *J Supercrit Fluids* 128:121–127. <https://doi.org/10.1016/J.SUPFLU.2017.05.014>
- Nalawade SP, Picchioni F, Janssen LPBM (2006) Supercritical carbon dioxide as a green solvent for processing polymer melts: processing aspects and applications. *Prog Polym Sci* 31:19–43. <https://doi.org/10.1016/J.PROGPOLYMSCI.2005.08.002>
- Nguyen P, Carey JW, Viswanathan HS, Porter M (2018) Effectiveness of supercritical-CO₂ and N₂ huff-and-puff methods of enhanced oil recovery in shale fracture networks using microfluidic experiments. *Appl Energy* 230:160–174. <https://doi.org/10.1016/J.APENERGY.2018.08.098>
- Ogden S, Bodén R, Do-Quang M et al (2014) Fluid behavior of supercritical carbon dioxide with water in a double-Y-channel microfluidic chip. *Microfluid Nanofluidics* 17:1105–1112. <https://doi.org/10.1007/s10404-014-1399-6>
- Ohashi A, Sugaya M, Kim H-B (2011) Development of a microfluidic device for measurement of distribution behavior between supercritical carbon dioxide and water. *Anal Sci* 27:567. <https://doi.org/10.2116/analsci.27.567>

- Ostmann S, Kähler CJ (2022) A simple projection photolithography method for low-cost rapid prototyping of microfluidic chips. *Microfluid Nanofluidics* 26:24. <https://doi.org/10.1007/s10404-022-02531-5>
- Palde PB, Jamison TF (2011) Safe and efficient tetrazole synthesis in a continuous-flow microreactor. *Angew Chem Int Ed* 50:3525–3528. <https://doi.org/10.1002/anie.201006272>
- Park JI, Nie Z, Kumachev A et al (2009) A microfluidic approach to chemically driven assembly of colloidal particles at gas-liquid interfaces. *Angew Chem Int Ed* 48:5300–5304. <https://doi.org/10.1002/anie.200805204>
- Peng XF, Peterson GP (1996) Convective heat transfer and flow friction for water flow in microchannel structures. *Int J Heat Mass Transf* 39:2599–2608. [https://doi.org/10.1016/0017-9310\(95\)00327-4](https://doi.org/10.1016/0017-9310(95)00327-4)
- Phillips TW, Lignos IG, Macecizyk RM et al (2014) Nanocrystal synthesis in microfluidic reactors: where next? *Lab Chip* 14:3172–3180. <https://doi.org/10.1039/C4LC00429A>
- Pisanti P, Yeatts AB, Cardea S et al (2012) Tubular perfusion system culture of human mesenchymal stem cells on poly-L-lactic acid scaffolds produced using a supercritical carbon dioxide-assisted process. *J Biomed Mater Res A* 100A:2563–2572. <https://doi.org/10.1002/jbm.a.34191>
- Pohar A, Plazl I (2008) Laminar to turbulent transition and heat transfer in a microreactor: mathematical modeling and experiments. *Ind Eng Chem Res* 47:7447–7455. <https://doi.org/10.1021/ie8001765>
- Qian J, Li X, Wu Z et al (2019) A comprehensive review on liquid-liquid two-phase flow in microchannel: flow pattern and mass transfer. *Microfluid Nanofluidics* 23:116. <https://doi.org/10.1007/s10404-019-2280-4>
- Qin K, Wang K, Luo R et al (2018a) Dispersion of supercritical carbon dioxide to [Emim][BF₄] with a T-junction tubing connector. *Chem Eng Process Process Intensif* 127:58–64. <https://doi.org/10.1016/J.CEP.2018.03.003>
- Qin N, Wen JZ, Chen B, Ren CL (2018b) On nonequilibrium shrinkage of supercritical CO₂ droplets in a water-carrier microflow. *Appl Phys Lett* 113:33703. <https://doi.org/10.1063/1.5039507>
- Quitain AT, Mission EG, Sumigawa Y, Sasaki M (2018) Supercritical carbon dioxide-mediated esterification in a microfluidic reactor. *Chem Eng Process Process Intensif* 123:168–173. <https://doi.org/10.1016/J.CEP.2017.11.002>
- Reverchon E, Adami R (2006) Nanomaterials and supercritical fluids. *J Supercrit Fluids* 37:1–22. <https://doi.org/10.1016/j.supflu.2005.08.003>
- Roig Y, Marre S, Cardinal T, Aymonier C (2011) Synthesis of exciton luminescent ZnO nanocrystals using continuous supercritical microfluidics. *Angew Chem Int Ed* 50:12071–12074. <https://doi.org/10.1002/anie.201106201>
- Sahena F, Zaidul ISM, Jinap S et al (2009) Application of supercritical CO₂ in lipid extraction—a review. *J Food Eng* 95:240–253. <https://doi.org/10.1016/J.JFOODENG.2009.06.026>
- Shekunov BY, Chattopadhyay P, Seitzinger J, Huff R (2006) Nanoparticles of poorly water-soluble drugs prepared by supercritical fluid extraction of emulsions. *Pharm Res* 23:196–204. <https://doi.org/10.1007/s11095-005-8635-4>
- Singh UK, Vannice MA (2001) Kinetics of liquid-phase hydrogenation reactions over supported metal catalysts—a review. *Appl Catal A Gen* 213:1–24. [https://doi.org/10.1016/S0926-860X\(00\)00885-1](https://doi.org/10.1016/S0926-860X(00)00885-1)
- Sirsi SR, Borden MA (2009) Microbubble compositions, properties and biomedical applications. *Bubble Sci Eng Technol* 1:3–17. <https://doi.org/10.1179/175889709X446507>
- Sollier E, Murray C, Maoddi P, Di Carlo D (2011) Rapid prototyping polymers for microfluidic devices and high pressure injections. *Lab Chip* 11:3752–3765. <https://doi.org/10.1039/C1LC20514E>
- Song H, Chen DL, Ismagilov RF (2006) Reactions in droplets in microfluidic channels. *Angew Chem Int Ed Engl* 45:7336–7356. <https://doi.org/10.1002/anie.200601554>
- Stratmann A, Schweiger G (2002) Fluid phase equilibria of ethanol and carbon dioxide mixtures with concentration measurements by Raman spectroscopy. *Appl Spectrosc* 56:783–788. <https://doi.org/10.1366/000370202760077531>
- Tang Q, Wang T (2005) Preparation of silica aerogel from rice hull ash by supercritical carbon dioxide drying. *J Supercrit Fluids* 35:91–94. <https://doi.org/10.1016/j.supflu.2004.12.003>
- Taylor LT (2009) Supercritical fluid chromatography for the 21st century. *J Supercrit Fluids* 47:566–573. <https://doi.org/10.1016/j.supflu.2008.09.012>
- Teh S-Y, Lin R, Hung L-H, Lee AP (2008) Droplet microfluidics. *Lab Chip* 8:198–220. <https://doi.org/10.1039/B715524G>
- Theberge AB, Courtois F, Schaeferli Y et al (2010) Microdroplets in microfluidics: an evolving platform for discoveries in chemistry and biology. *Angew Chem Int Ed* 49:5846–5868. <https://doi.org/10.1002/anie.200906653>
- Tiggelaar RM, Benito-López F, Hermes DC et al (2007) Fabrication, mechanical testing and application of high-pressure glass microreactor chips. *Chem Eng J* 131:163–170. <https://doi.org/10.1016/J.CEJ.2006.12.036>
- Trachsel F, Hutter C, von Rohr PR (2008) Transparent silicon/glass microreactor for high-pressure and high-temperature reactions. *Chem Eng J* 135:S309–S316. <https://doi.org/10.1016/J.CEJ.2007.07.049>
- Trachsel F, Tidona B, Desportes S, Rudolf von Rohr P (2009) Solid catalyzed hydrogenation in a Si/glass microreactor using supercritical CO₂ as the reaction solvent. *J Supercrit Fluids* 48:146–153. <https://doi.org/10.1016/J.SUPFLU.2008.09.026>
- Tumarkin E, Il PJ, Nie Z, Kumacheva E (2011) Temperature mediated generation of armoured bubbles. *Chem Commun* 47:12712–12714. <https://doi.org/10.1039/C1CC14545B>
- Tyskiewicz K, Konkol M, Rój E (2018) The application of supercritical fluid extraction in phenolic compounds isolation from natural plant materials. *Molecules* 23:2625
- Urakawa A, Trachsel F, von Rohr PR, Baiker A (2008) On-chip Raman analysis of heterogeneous catalytic reaction in supercritical CO₂: phase behaviour monitoring and activity profiling. *Analyst* 133:1352–1354. <https://doi.org/10.1039/B808984C>
- Uwineza PA, Waśkiewicz A (2020) Recent advances in supercritical fluid extraction of natural bioactive compounds from natural plant materials. *Molecules* 25:3847
- Wang K, Lu YC, Xia Y et al (2011) Kinetics research on fast exothermic reaction between cyclohexanecarboxylic acid and oleum in microreactor. *Chem Eng J* 169:290–298. <https://doi.org/10.1016/j.cej.2011.02.072>
- Watts P, Haswell SJ (2005) The application of micro reactors for organic synthesis. *Chem Soc Rev* 34:235–246. <https://doi.org/10.1039/B313866F>
- Weibel GL, Ober CK (2003) An overview of supercritical CO₂ applications in microelectronics processing. *Microelectron Eng* 65:145–152. [https://doi.org/10.1016/S0167-9317\(02\)00747-5](https://doi.org/10.1016/S0167-9317(02)00747-5)
- Williams JR, Clifford AA, Al-Saidi SHR (2002) Supercritical fluids and their applications in biotechnology and related areas. *Mol Biotechnol* 22:263. <https://doi.org/10.1385/MB:22:3:263>
- Yahya NA, Attan N, Wahab RA (2018) An overview of cosmetically relevant plant extracts and strategies for extraction of plant-based bioactive compounds. *Food Bioprod Process* 112:69–85. <https://doi.org/10.1016/J.FBP.2018.09.002>
- Yang F, Li Y, Chen Z et al (2009) Superparamagnetic iron oxide nanoparticle-embedded encapsulated microbubbles as dual contrast agents of magnetic resonance and ultrasound imaging. *Biomaterials* 30:3882–3890. <https://doi.org/10.1016/J.BIOMATERIALS.2009.03.051>
- Yao C, Zhu K, Liu Y et al (2017) Intensified CO₂ absorption in a microchannel reactor under elevated pressures. *Chem Eng J* 319:179–190. <https://doi.org/10.1016/J.CEJ.2017.03.003>

- Yen BKH, Günther A, Schmidt MA et al (2005) A Microfabricated gas-liquid segmented flow reactor for high-temperature synthesis: the case of CdSe quantum dots. *Angew Chem Int Ed* 44:5447–5451. <https://doi.org/10.1002/anie.200500792>
- Zheng X, Mahabadi N, Yun TS, Jang J (2017) Effect of capillary and viscous force on CO₂ saturation and invasion pattern in the microfluidic chip. *J Geophys Res Solid Earth* 122:1634–1647. <https://doi.org/10.1002/2016JB013908>
- Zhu W, Fan Y, Zhang C et al (2018) Impregnation of viscose substrate with nicotinamide in supercritical carbon dioxide. *Text Res J*. <https://doi.org/10.1177/0040517518813683>

Publisher's Note Springer Nature remains neutral with regard to jurisdictional claims in published maps and institutional affiliations.

Springer Nature or its licensor holds exclusive rights to this article under a publishing agreement with the author(s) or other rightsholder(s); author self-archiving of the accepted manuscript version of this article is solely governed by the terms of such publishing agreement and applicable law.